Journal of Applied Fluid Mechanics, Vol. 18, No. 4, pp. 850-863, 2025.
Available online at www.jafmonline.net, ISSN 1735-3572, EISSN 1735-3645.
https://doi.org/10.47176/jafm.18.4.3002

Reacting Flow Characteristics of Wall-mounted Ramps in Strut-injection Scramjet Combustors under Varying Hydrogen Jet Pressures

A. Antony Athithan[1] and S. Jeyakumar[2†]

[1] *Faculty of Engineering, Lincoln University College, Petaling Jaya 47301, Malaysia*
[2] *CFD Center, Mechanical Engineering, Kalasalingam Academy of Research and Education, Krishnankoil, India*

†*Corresponding Author Email: s.jeyakumar@klu.ac.in*

ABSTRACT

Implications of hydrogen pressure injection variances from strut injectors in a supersonic reacting flow domain have been a focus of this study. A numerical investigation is performed using Reynolds Averaged Navier Stokes (RANS) equations in combination with the Shear Stress Transport (SST) k-ω turbulence model to understand flow mechanics at supersonic combustion. Under varying fuel jet pressures, the impact of dual ramps symmetrically placed at the scramjet combustor walls behind a strut injection is computationally investigated. The effect of hydrogen injection pressure variations in scramjet combustors is explored based on essential features including shock pattern, static pressure fluctuations, and static temperature throughout the combustor. The numerical outcomes are confirmed by experimental data and lie within a reasonable range, indicating that the simulation method may be applied to further study. Variation in fuel injection pressures affects supersonic combustion phenomena in hypersonic vehicles, according to the findings of this study. A rise in the hydrogen jet pressure accelerates flow downstream of the injector and reduces the intensity of shock wave interactions in ramp-based scramjet combustors. In addition, the present research demonstrates that an increase in hydrogen jet pressure, P5, in reactive supersonic airflow accelerates mixing and combustion, with a minimal overall pressure loss of 17% in the combustor, achieved within a shortened length of approximately 52% compared to the DLR model.

Article History

Received July 24, 2024
Revised October 17, 2024
Accepted October 31, 2024
Available online February 4, 2025

Keywords:

Strut injector
Ramps
Scramjet
Supersonic combustion
Hydrogen jet pressure

1. INTRODUCTION

Supersonic combustion is the most prominent research in high-speed propulsion (Viaud & Mestre, 1966; Ben-Yakar & Hanson, 2001; Clark & Bade Shrestha, 2015) A scramjet engine's fuel injection system is essential for enhancing both the fuel-air mixing performance and entire incineration. Scramjet combustor's short airflow residence time necessitates a significant flame-holding mechanism. Scramjet uses hydrogen as a viable fuel because its features include quick interaction with air, easy flammability, effective combustion, non-pollution, and so on (Cecere et al., 2014).

Complete hydrogen fuel combustion is required, based on an effective fuel injection system that may increase the fuel and air effective mixing & complete combustion with minimum total pressure loss. Flush wall injection (Goyne et al., 2001; Tahani et al., 2016), cavities (Jeyakumar et al., 2006, 2017, 2018; Assis et al., 2019; Wang et al., 2020), pylons(Doster et al., 2007; Gruber et al., 2008; Lee, 2012), strut-based injectors (Génin & Menon, 2010; Soni & De, 2017; Aravind & Kumar, 2019; Suneetha et al., 2019; Antony Athithan et al., 2021; Athithan et al., 2021; Jeyakumar et al., 2021; Lakka et al., 2021), etc., are the choices for addressing the concerns stated above while also limiting to overall total pressure loss. On a DLR scramjet combustor, Waidmann et al. (1994, 1995) executed a number of experiments employing a strut fuel injection system. Combustion tests are accomplished in a variety of circumstances, including pressure, temperature, and so on. Through the utilization of flamelet model, Oevermann (2000) carried out computational explorations on scramjet combustors in 2D and corroborated flow parameters by cross-referencing them with experimental findings published by DLR (Guerra et al., 1991; Waidmann et al., 1995). Building on Oevermann's work, numerous researchers (Génin & Menon 2010; Fureby et al., 2014; Xue et al. 2017) employed the strut injector for emulating supersonic

combustion and analyzing shock wave interactions induced by strut for augmenting air-fuel blending and combustion in scramjet engines. This finding sparked the present investigation, which aims to enhance the above-mentioned objectives using hydrogen injection in addition to strut injectors.

Bruno and Ingenito (2021) studied the jet penetration into a supersonic flow and suggested that the momentum flux ratio should be greater than one for rapid and effective fuel jet penetration into a high-momentum airstream. Li and Gu (2022) researched cavity-type scramjet combustors using ethylene fuel and revealed that the lack of fuel in the shear layer zone is caused by unstable flame near the jet stream wake region. As a result, the flame extinguishes at the jet stream wake region and is reignited at the downstream shear layer, which aids in the propagation of the combustion waves. Through increased injection pressure and airflow total temperature, Xi et al. (2022), experimental studies in a supersonic flow of Mach 2.5 led to enhanced mixing efficiency and shorter ignition delay times. Moreover, oblique shocks trigger auto-ignition, which later extends upstream to the recirculating zone.

The numerical analysis conducted by Neill and Pesyridis (2017) on a twin-strut supersonic combustor indicates that strut injectors enhance pressure restoration more effectively than transverse injection, with a negligible impact on mixture efficiency and percentage fuel depletion. According to Qin et al. (2019), an innovative strut injector is used to stabilize flame in a reacting supersonic flow. Also, the innovative strut base generates intense shock waves that result in a high temperature and pressure zone and increased total pressure loss. Thakur et al. (2021), studied the fuel and air injection using a rearward step flame holder in a flow field of Mach 1.6. The authors reported that the two air jets surrounding the fuel injection provide enhanced combustion efficiency.

A numerical analysis of the impact of various injector models on the mixing behaviour of planar supersonic jets has been presented by Gerlinger and Bruggemann (2000). The authors examined a variety of computed performance indicators to analyze variations in injection Mach number and lip thickness. Results revealed that minor changes in injector length and height had less of an impact on total pressure loss than lip thickness. A 17% greater loss in total pressure was caused by the 1.6 mm increase in lip height.

Huang's study (2015) explored the influence of the strut edge radius, half-angle, and placement in relation to the inlet on the combustion regime of a scramjet combustor. Since shocks interact with enhanced boundary layer features, increasing the strut edge radius improves the flow separation regime. The length of the combustor increases along with a linear improvement in combustion efficiency. Although many of the studies mentioned above focused on the supersonic region of the combustor, the influence of different strut injecting configurations, shock–shear layer interactions generated by struts, and its characteristics, numerous flow properties still need to be investigated to accomplish flame stability and optimize the scramjet performance.

The combustion properties of scramjets at various flight dynamic pressures have been examined by Zhang et al. (2023). The author concluded that as the starting temperature increases, reducing the flight dynamic pressure enhances fuel mixing and reduces ignition delay. Kerosene fuel is utilized in these engines, therefore this finding is quite significant. Thus, enhancing fuel mixing efficiency is essential to facilitating the combustion process. The high-quality syngas production using gliding arc plasma has been studied by Liu and Zhu (2024). Chang et al. (2024) examine affinity laws for multistage pumps under gas-liquid conditions, showing strong applicability with over 0.9 accuracy. The reacting and non-reacting flow analyses were performed in previous studies using computational methods (Gao et al., 2024; Muhammed et al., 2024).

Fuel infusion before the ramp is favourable for spreading the fuel, according to Moorthy et al. (2014) studied the consequences of ramp cavities on a hydrogen-fueled supersonic combustor. As a result of the ramps' significant influence on the flow over the cavities, fuel is prevented from spreading by wakes and other flow features. The ramp flow aids in spreading the fuel, making H_2 infusion in the midst of ramps advantageous. Due to the interaction of the ramp's front-end shock with the recirculation zone complying with each stage, ramps situated on either a higher or lower floor prohibit the combustor from reaching its maximum height. High-temperature, low-velocity recirculation zones in cavities serve as flame stabilizers. Furthermore, the 3D flow area produced by discrete ramps on top & lower floors, along with the instability of the cavity shear layer, enhances mixing efficiency.

Computational study by Abu-Farah et al. (2014) on multi-staged H_2 injection in a 3D combustor revealed that employing three stages of H_2 injection via the strut, wall 1, and wall 2 causes roughly twice as many total pressure losses as using a single stage through the strut. The computational study by Choubey et al. (2023) on the scramjet combustor cavity floor H_2 fuel injection technique revealed that the cavity floor injection has been shown to stabilize the flame at Mach values of 1.5, 2.5, and 3.5. The prediction shows that the cavity floor injection controls shock wave propagation in the downstream direction, which may cause the engine to shut off, even if cavity floors with other injection methods are suitable for supersonic reaction flow configurations.

The key findings of the study suggested by Liu et al. (2023) on increasing the distance of the cavity to the backward facing step in a scramjet combustor can improve mixing efficiency, reduce combustion temperature, and enhance combustion stability. These results demonstrate the high reliability of simulation results since they are based on simulations that successfully recreate the structure of flows & flame stabilization modes. Numerical analysis performed by the authors (Antony Athithan et al., 2021; Athithan et al., 2021) on strut-based combustors with double ramps improves the propagation of H_2 mass fraction in the transverse direction of the combustor. Additional reflection of shocks and their collisions caused

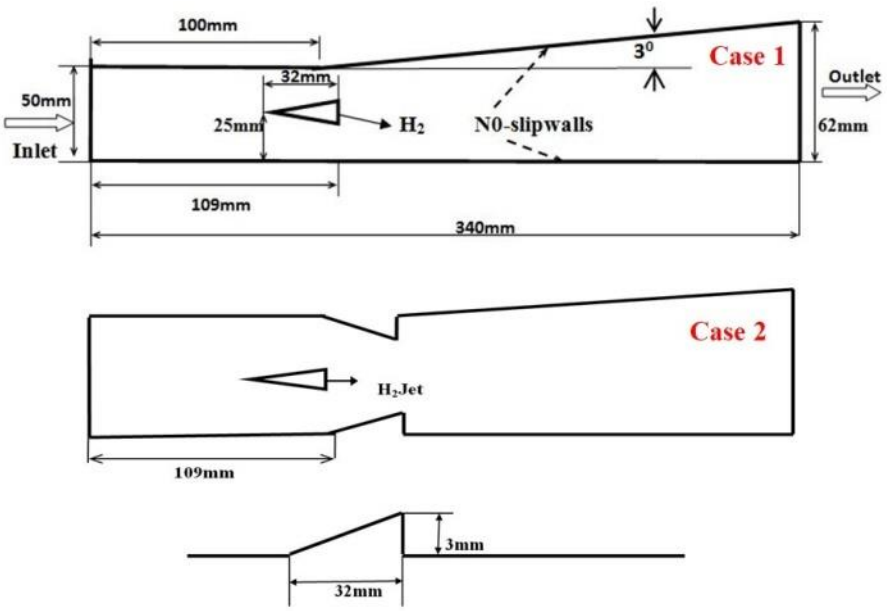

Fig. 1 Sketch of DLR combustors model of scramjet

ignition delay and enhanced combustion in the scramjet combustor.

From the open literature, the performance of various fuel injection schemes in supersonic reacting flow fields to enhance mixing and combustion is detailed. However, the influence of H_2 jet pressure variation in a supersonic flow domain with wall-mounted ramps in the combustor of a scramjet has not been reported. In this regard, the current work investigates the impact of H_2 jet pressure variations fed by strut injectors with symmetrical wall ramps incorporated within a 2D combustor in a reacting flow environment. RANS equation is used in this study, together with SST k-ω turbulence model, and a single-step H_2-air combustion reaction. Findings, which include flow characteristics and combustor performance parameters including mixing and combustion efficiencies, and loss in overall pressure may aid in the development of parallel injection techniques in a combustor.

2. NUMERICAL METHODOLOGY

The computational study on 2D scramjet combustor is analyzed using commercial software namely, ANSYS Fluent. In the current study, the flow region is solved with a 2D compressible RANS expression and a density-type double precision solver. This expression is critical because it produces precise outputs with coarse grids and resolves steady flow more effectively than other models (Qin et al., 2019). An SST k-ω model with typical parameters is adopted to resolve the turbulent flow field (Ou et al., 2018; Zhang et al., 2018; Thakur et al., 2021). The fluid flow interactions are efficiently predicted by the SST k-ω model (Jeyakumar et al., 2021). To obtain a precise solution with constant convergence properties (Gerlinger & Bruggemann, 2000), the combination of the Advection Flux Splitting Method (AUSM) and second-order upwind scheme (SOU) is utilized for spatial discretization. Calculation of thermal conductivity and viscosity is carried out by applying the mass-weighted-mixing law, and the stream is regarded as a perfect gas. RANS expressions implemented in the current study are obtained from computational studies (Ivanova et al., 2013; Huang, 2014; Athithan & Jeyakumar, 2022) of many researchers.

2.1 Combustion Modeling

In supersonic combustion simulations, equations describing the transport of different chemical species and models for eddy-dissipation are employed (Magnussen & Hjertager, 1976). Interaction between turbulence and chemical reactions is resolved using an eddy-dissipation model, which aligns well with experimental findings. The utilization of a single-step H_2-air reaction is more effective than a multi-step model (Huang et al., 2012) in evaluating the overall performance of a combustor based on various parameters (Kumaran & Babu, 2009) and hence, it is employed in this research to assess the combustor's whole effectiveness, while keeping the computational cost low. The corresponding reaction expression is provided below:

$$2H_2 + O_2 \rightarrow 2H_2O \quad (1)$$

The solutions are considered to be converged when the residuals have dropped significantly greater than 3 orders of magnitude and the variation of inflow & outflow mass flux is lower than 0.001kg/s. This implies that the simulation has reached a state where the results are stable and no significant changes are expected even if the calculation is continued further.

2.2 Computational Region

A two-dimensional line diagram of the DLR scramjet combustor model experimented by Waidmann et al. (1994, 1995) is illustrated in Fig. 1. At, 2.0 Mach, air enters the combustor, while H_2 is infused at sonic velocity parallel to the flow direction from the strut. The cross-section of the combustor intake is 40x50 mm up to a length

Table 1 Boundary conditions implemented in the model

Parameters	Air	H_2 Injection (cases)			
		Strut	P=1bar	P=3bar	P=5bar
Ma	2.0	1.0	1.0	1.0	1.0
u (m/s)	706	191	191	191	191
T (K)	540	300	300	300	300
P (bar)	1.0	1.0	1.0	1.0	1.0
ρ (kg/m^3)	1.002	0.097	0.097	0.097	0.097
YO_2	2.32	0	0	0	0
YH_2	0	1	1	1	1
YH_2O	0.032	0	0	0	0
YN_2	0.736	0	0	0	0

of 100 mm, after which the top wall is diverged by 3o degrees towards the exit. The strut is positioned at the combustor's centre, radial to flow direction (Y=25mm) and 77mm from the inlet. The length of the strut is 32mm and features 6o degrees half divergence angle. H2 is infused through 15 orifices with a diameter of 1mm from the strut's base. Experimental information on the DLR model is disseminated by (Guerra et al., 1991; Waidmann et al., 1994). The model is based on operational parameters obtained from references (Guerra et al., 1991; Waidmann et al., 1994). In this study, two ramps are symmetrically positioned at 109 mm from the entrance at the combustor walls behind of strut injector. DLR model is mentioned as the baseline model and varying hydrogen injection pressures in ramp combustor are compared to the baseline model in this study. Three hydrogen jet pressures of 1 bar, 3 bar, and 5 bar, are indicated as P1, P3, and P5 respectively, and the baseline model as strut. The scramjet engine's operational parameters are identical for all the simulations.

2.3 Operating Conditions

Operating conditions have an impact on the solutions to computational problems. At Mach 2, supersonic air enters an isolator, while various hydrogen jet pressures such as 1 bar, 3 bar, and 5 bar are fed from the strut injector. Table 1 represents operating scenarios at the combustor inlet and exit. Dirichlet condition is used to define air and fuel at the combustor entrance, while Neumann condition is defined for domain outflow. The pressure outlet boundary condition is mentioned at the computational domain's outlet. All physical characteristics are extended from interior cells since flow is supersonic (Huang et al., 2010).

2.4 Grid Independency Test

Flow region in the model is resolved using an unstructured grid in this research. The grid resolution is optimized using three different grids, resulting in improved numerical results while lowering processing cost and time. For the grid independency study, coarse (146146), medium (191607), & fine (290112) grid sizes are tested. Y+ value of the whole flow field is less than 1.0, which corresponds to 0.001 mm height of the first-row cell as shown in Fig. 2a. Figure 2b depicts the grid independence research of the double ramp model. Following the convergence study, it is revealed that static pressure values offer a variation of less than 1% for all mesh sizes, indicating that nil subsequent error analysis is

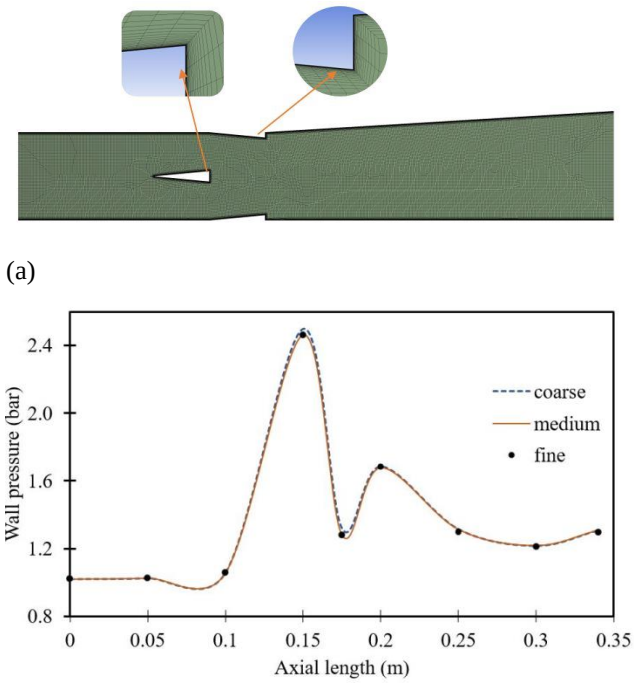

Fig. 2 (a) Meshed computational domain (b) Grid independency study

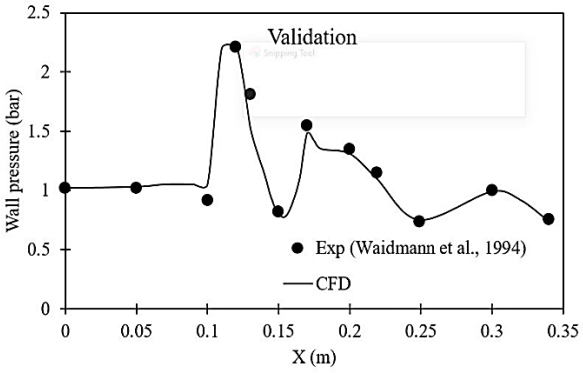

Fig. 3 Wall pressure dispersion of experimental and numerical results

necessary to demonstrate grid convergence. Furthermore, medium and fine grids produce about the same profile downstream of the strut. As a result, the medium-sized mesh is utilized to diminish the computing period.

2.5 Validation

Waidmann et al. (1994, 1995) documented the DLR experiment findings, which are displayed in Fig. 3. Computational output of pressures over walls along the axis is compatible with the experimental measurements. Forecast numerical data by Oevermann (2000) & Huang (2015) are incorporated in the centerline velocity distribution of the combustor, Y=25 mm, Fig. 4., for comparison. The fuel stream decelerates at the combustion area, where shock interfaces with shears, as shown in the velocity profile. A virtually uniform profile with a slight decrease in velocity appears down the combustor, at x=0.18m from the combustor entrance, as flow accelerates.

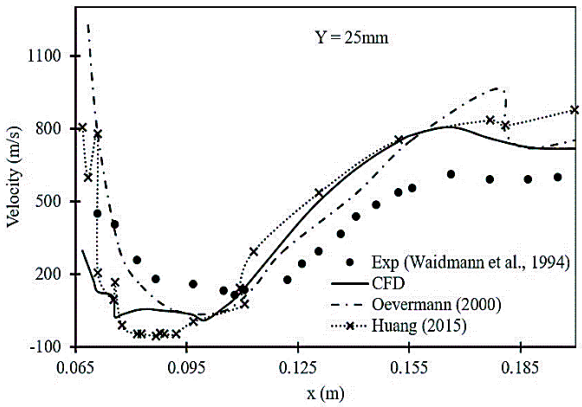

Fig. 4 Centerline velocity dispersion of numerically simulated Vs experiments results

Simulation findings are qualitatively consistent with experimental data are agree with the results of references (Oevermann, 2000; Huang, 2015). This analysis achieves a significant acceleration downstream and lowers velocity values.

3. RESULT AND DISCUSSION

A computational analysis of a DLR strut scramjet combustor having a downstream double ramp for various fuel injection pressures in a reaction flow field is presented in subsequent sections. Numerical shadowgraph images for combustor models with varying fuel injection pressures are depicted in Fig. 5. For all the cases, oblique shocks from the lead of the strut are denoted as leading-edge shock waves, whereas for double ramp cases, additional shocks from the forefront of ramps are created which are denoted as ramp-related shock waves in shadowgraph images. The shock - boundary layer interaction are detailed in the reference (Huang et al., 2020). Shocks from the strut base and reflected shocks from combustor walls impact on hydrogen jet shear layer in the DLR scramjet model, which improves fuel stream shears mixing thickness and widens the combustion zone. For ramp case P1, boundary layer separation occurs upstream of ramps due to the interaction of shocks from the strut's tip and base, which interact with the combustor wall boundary layers and create lambda shock waves. The shocks at the aft end of ramps interact with the fuel stream behind the strut which widens the fuel jet and decelerates the flow to the downstream combustor. As hydrogen jet pressure rises to 3 bar, ramp case P3, strut's front edge shocks reflected exactly from the forefront of ramps & interacted with the trailing edge shock. These reflected shock waves impinge at the same location on the shear layer which progresses the width of the shear layer in the subsonic region and enhances the fuel-air mixing. In addition, more strong shock wave reflections and interactions could be observed with the shear layer and combustor walls. The absence of lambda shocks and flow separations is seen in the case of P3 compared to the case of P1. Further, for case P3, an acceleration of flow is noted downstream of ramps in the combustor compared to case P1. For the ramp case P5, the reflected leading-edge shocks from the strut travel along with the ramp-related

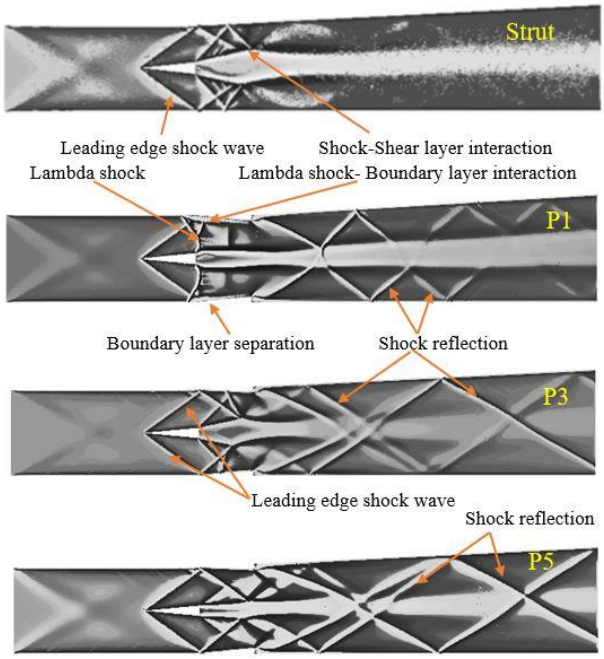

Fig. 5 Numerical shadowgraph of DLR strut-based scramjet combustor with various injection pressures

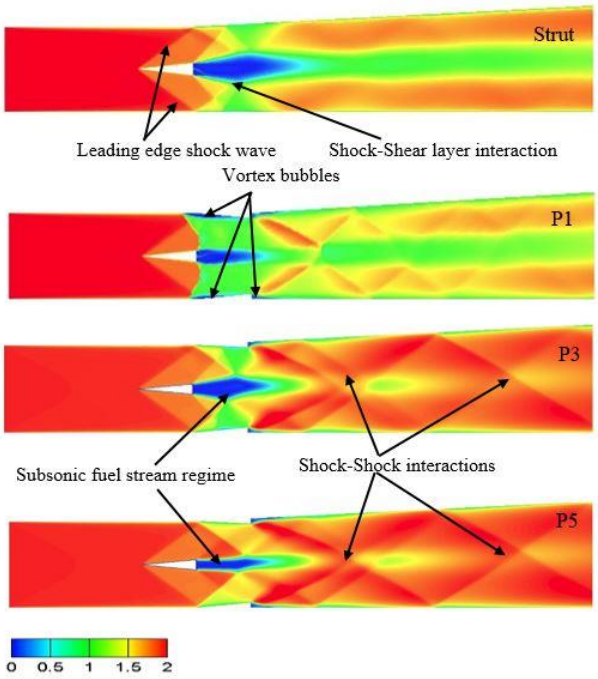

Fig. 6 Mach contour comparison of DLR strut scramjet combustor model with various injection pressures

shock waves with high intensity & impinge on fuel stream shears. More shocks from the ramp trailing edge and its reflections interact with the downstream shear layer with high intensity.

Mach contour of the flow in different scenarios of investigation is shown in Fig. 6. From the contours, it is noted that leading edge oblique shocks are created from the strut's forefront, and trailing edge shocks are seen at

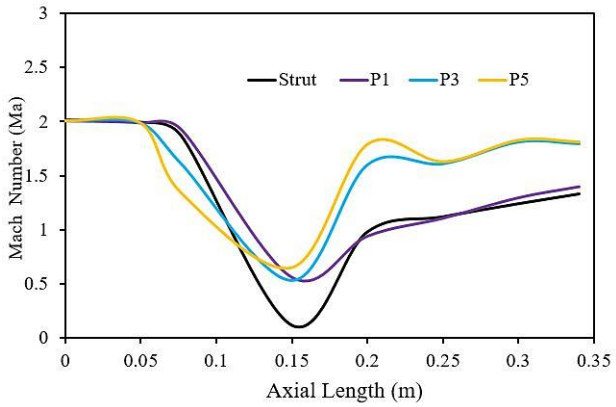

Fig. 7 Mach number variations along the axial length of combustor models

the aft end of the strut. In addition, additional shocks from the ramps interact with shock waves generated from the strut and hydrogen jet shear layers. For the ramp case P1, the boundary layer separation occurs over the ramps which creates a subsonic region on both sides of the strut injector that enhances air-fuel mixing. Shocks from the trailing edge of ramps and their reflections downstream of the combustor interact with the hydrogen stream shear layer which enhances the subsonic area at the mid-line of the combustor. Mach number variations along an axial combustor length are represented in Fig. 7. It is seen that flow is subsonic downstream of the strut where the subsonic region is created. An increase in H_2 jet pressures, case P3 and case P5 reduces the subsonic region at the vicinity of the strut and accelerates core flow downstream of ramps in the combustor.

Figure 8 compares the recirculation regions of the DLR model downstream of the strut and ramps for an increase in fuel injection pressures. In the strut case, a large vortex zone is observed behind the injector. However, the size of the recirculation zone varies with the strut ramp combustor of increasing hydrogen jet pressures.

For the ramp case P1, small vortices are seen at the boundary layer separation region upstream & downstream of ramps, which augment the mixing of air-fuel and enhance combustion. Moreover, the size of the vortices diminishes downstream of the strut injector due to the compressive nature in the vicinity of the strut ramp region. As hydrogen jet pressure increases, in the case of P3, counter-rotating vortices are observed downstream of the strut injector and flow separation could not be seen upstream of the ramps. Further, a rise in injection pressure, case P5, confines the recirculation region of the hydrogen jet downstream of the strut. This may be due to higher injection pressure which provides finer fuel particles that could enhance mixing and combustion at the molecular level with the incoming supersonic air stream within a short distance.

3.1 Bottom Wall Pressures

Figure 9 depicts pressure changes at the lower wall and midline of the combustor. For the DLR scramjet model, peak static pressure is recorded at X=0.13m and wavy patterns of pressure variations are due to shock interactions with lower wall boundary layers in the

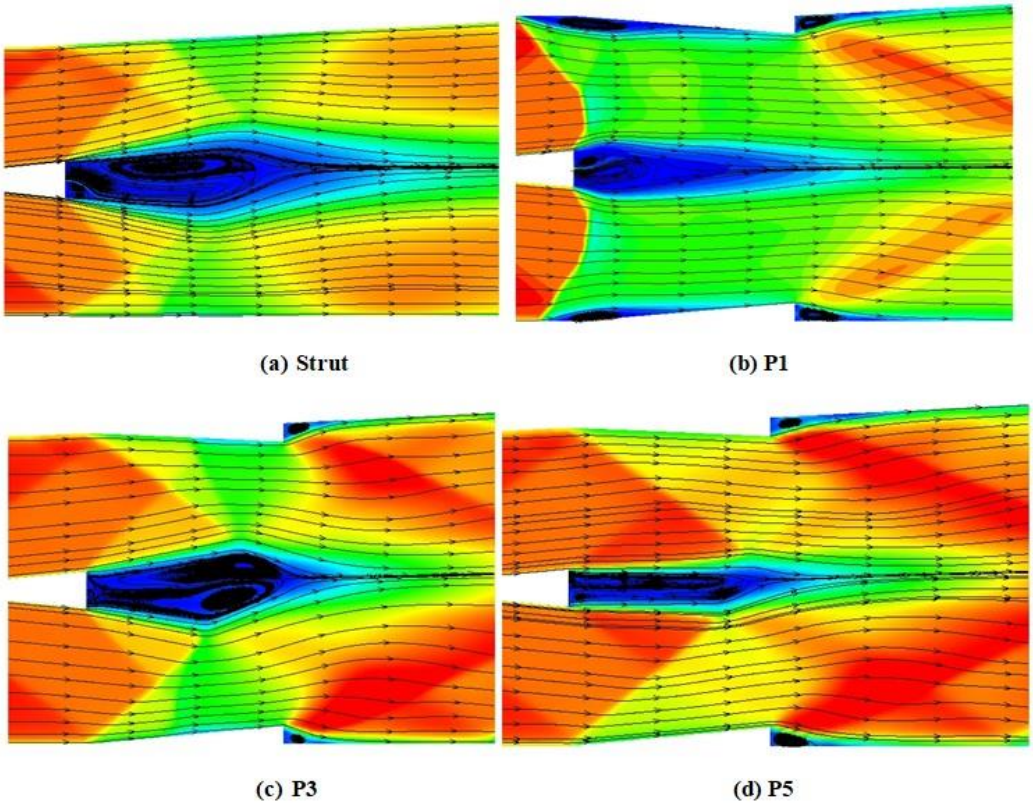

Fig. 8 Recirculation regions of DLR strut scramjet combustor model with various injection pressures

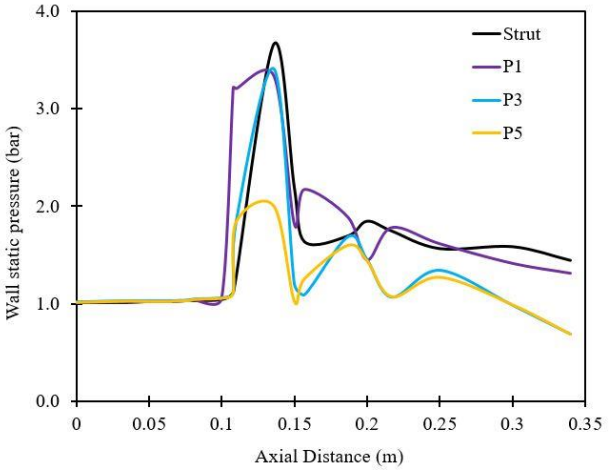

(a)

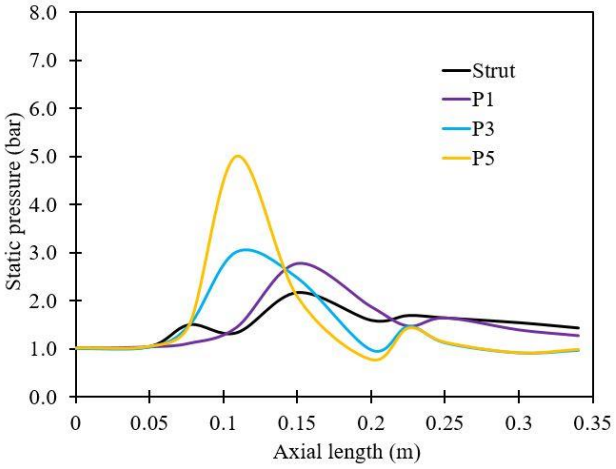

(b)

Fig. 9 (a) Wall static and (b) Centerline static pressure distribution of DLR strut scramjet combustor model with various injection pressures

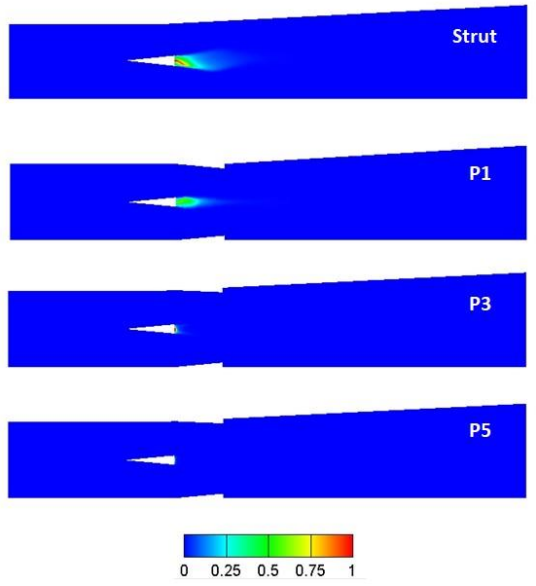

(a)

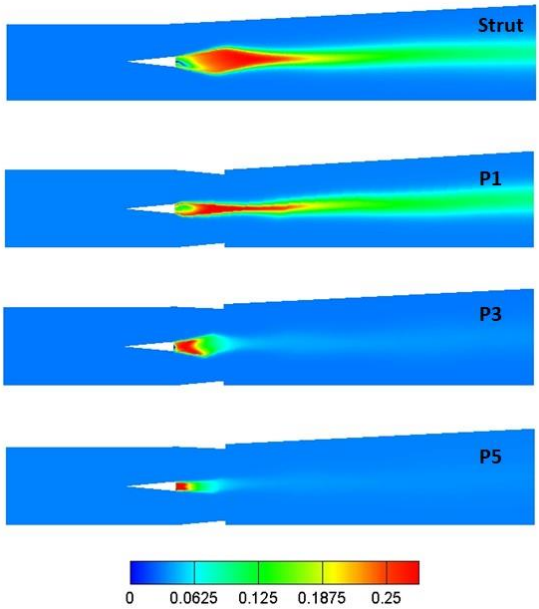

(b)

Fig. 10 Contours of (a) H_2 and (b) H_2O mass fraction along with combustor models with various injection pressures.

combustor. For ramp case P1, a peak static pressure curve is observed at the ramp due to shock-boundary interaction creating a separation of the flow region. As the hydrogen jet pressure increases, in case P3 and case P5, the nature of peak static pressure decreases due to the acceleration of core flow over the ramp region which can be realized in Fig.7. For a ramp with an injection pressure of P = 5 bar, the maximum centerline static pressure is observed at the base of strut injector and decreases along flow direction compared to other cases due to acceleration of the mainstream that is represented in Fig. 9(b).

Figure 9 depicts pressure changes at the lower wall and midline of the combustor. For the case 1 model, peak static pressure is recorded at X=0.13m and wavy patterns of pressure variations are due to shock interactions with lower wall boundary layers in the combustor. For ramp case P1, a peak static pressure curve is observed at the ramp due to shock-boundary interaction creating a separation of the flow region. As the hydrogen jet pressure increases, in case P3 and case P5, the nature of peak static pressure decreases due to the acceleration of core flow over the ramp region which could be realized in Fig.7. For a ramp with an injection pressure of P = 5 bar, the maximum centerline static pressure is observed at the base of strut injector and decreases along flow direction compared to other cases due to acceleration of the mainstream that is represented in Fig. 9(b).

3.2 Radicals of H_2 and H_2O

Due to the mass proportion of reactants & products throughout a combustor, the qualitative mixing behaviour of the H_2-air mixture combustion process employing a strut injector is investigated. Figures 10 and 11 depict the mass fraction of the reactants and products at three locations along stream-wise directions such as X= 0.15m, 0.2m, and 0.275m. Maximum H_2 mass fraction is observed

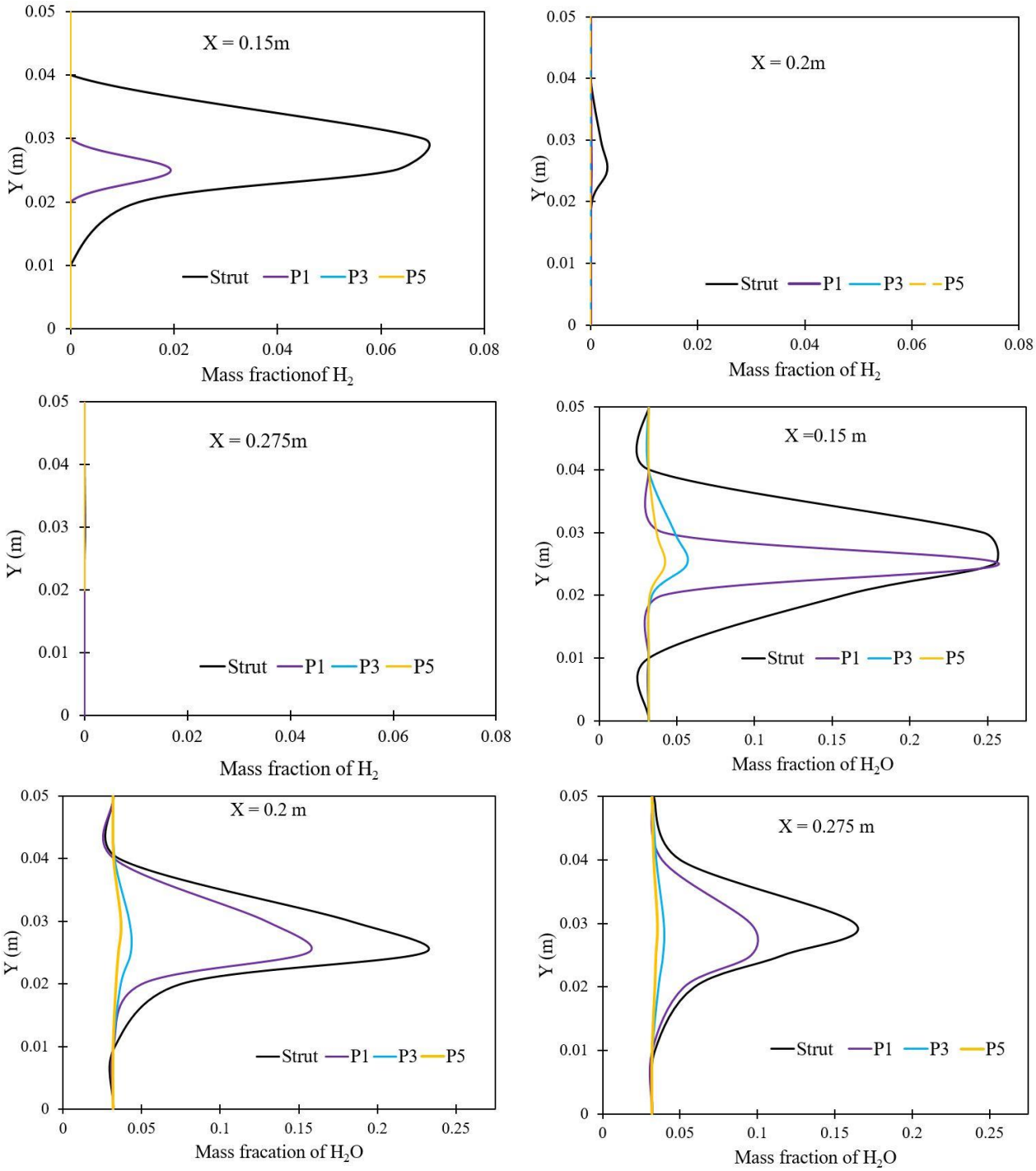

Fig. 11 Mass fraction of H_2 and water of DLR strut scramjet combustor model with various injection pressures

for strut case, at X= 0.15m whereas secondary peak is observed for ramp case P1. However, for case, P3 and case P5, the H_2 mass fraction is almost zero representing that with an axial length of the combustor for an increase in H_2 injection pressure is completely combusted and the products of the combustion reaction are observed from Fig. 11 (b). Also, the highest value for H_2O mass fraction is noted at X= 0.15m, for strut case and ramp case with P = 1 bar, indicating that shock-shear layer interactions downstream of the strut create an elongated subsonic regime that enhances mixing. An increase in the hydrogen jet pressure, case P3 and case P5, creates a finer hydrogen particle which accelerates mixing and combustion processes within a short combustor length.

Figure 12 shows the mass fraction of H_2 & H_2O along the flow direction of the combustor with increasing hydrogen jet pressures. The hydrogen mass fraction is higher for the DLR model and for the injection pressure P1. However, for the ramp cases P3 and P5, hydrogen fuel is completely consumed from the strut base indicating that an increase in injection pressure accelerates mixing & combustion compared to the normal injection case.

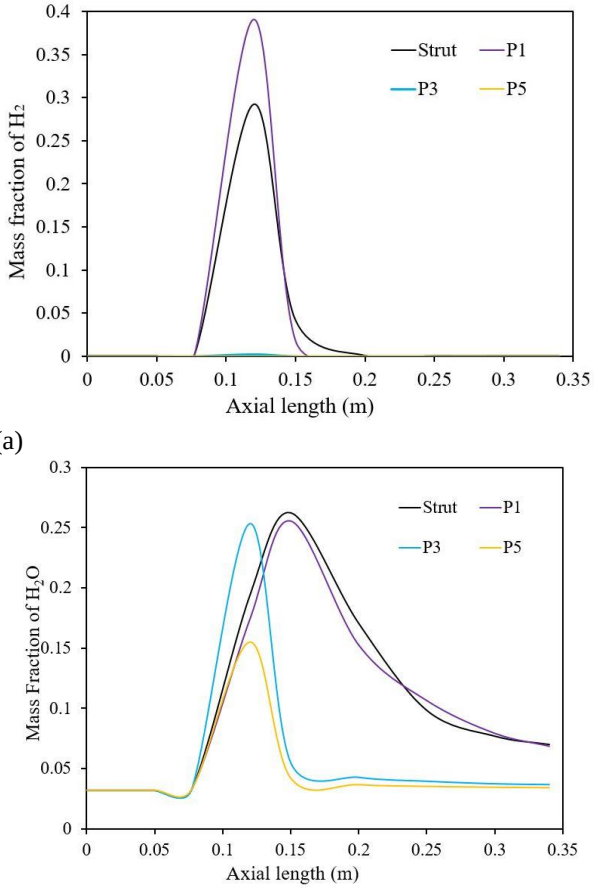

Fig. 12 Centerline Distribution of H_2 and H_2O Mass Fractions in Combustor Models: A Comparative Study

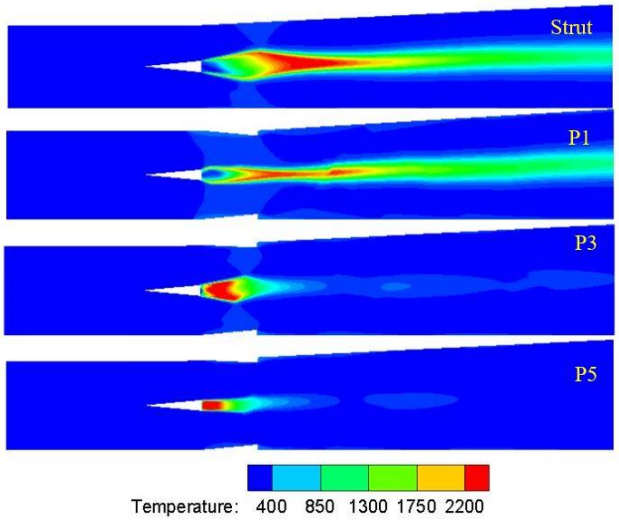

Fig. 13 Contour of the static temperature variation of combustor models with various injection pressures

3.3 Temperature

The magnitude of static temperature dispersal indicates the amount of heat emitted by the combustion process across a certain area within the combustor.

Figure 13 shows the static temperature contour and Fig.14 depicts the static temperature distribution of the scramjet combustor at various axial points such as

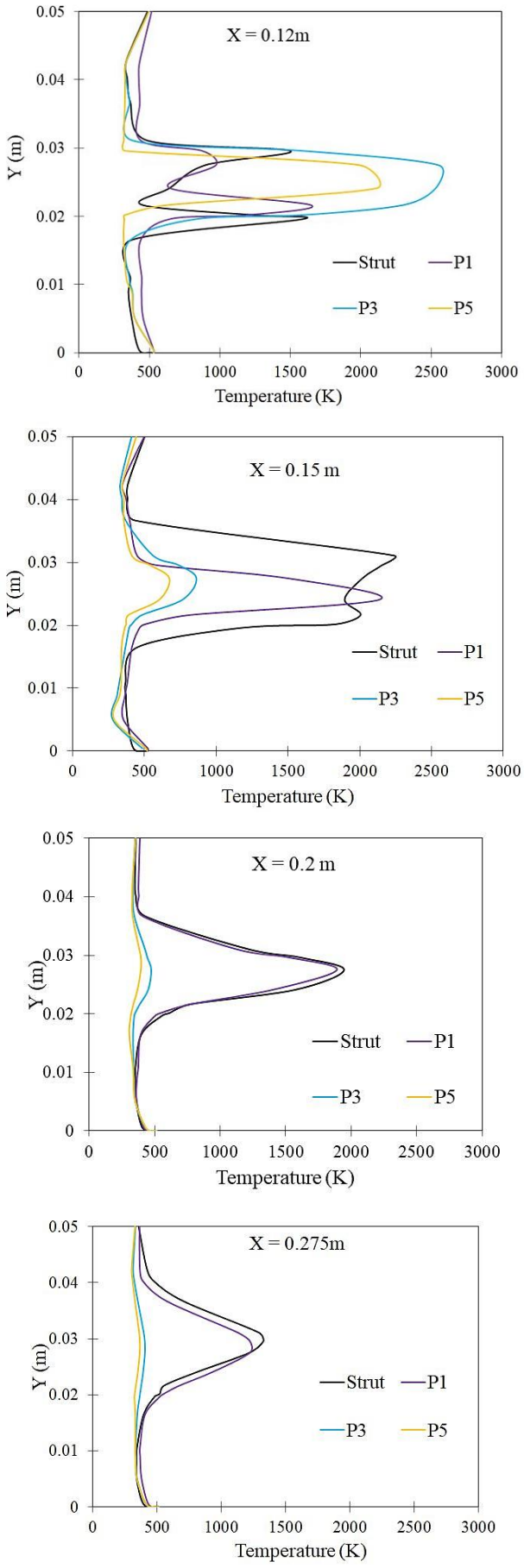

Fig. 14 Temperature variation across the DLR strut scramjet combustor models with various injection pressures

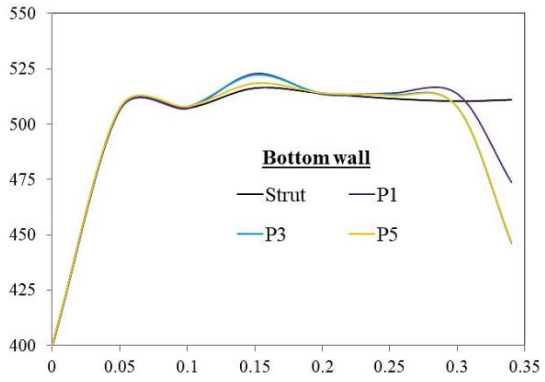

(a)

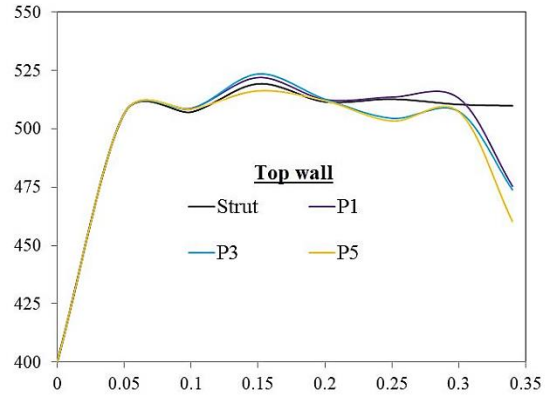

(b)

Fig. 15 Temperature variation along with the (a) bottom wall and (b) top wall of scramjet combustor models with various injection pressures

x =0.12m, 0.15m, 0.2m, and 0.275m for varied hydrogen jet pressures. At X =0.12m, a higher temperature of 2550K is noted for the case P3, it is due to high fuel injection pressure nearer to the strut base. However, in case P5, the complete combustion has been established within this axial length with a temperature of 2110 K which could be observed from Fig.14.At X= 0.15m, a peak temperature of 2200K and 2140 K is noted for the strut case and case P1, due to enhanced ignition delay compared to the case P3 and case P5. Further, the temperature distribution shows a similar profile for both strut case and ramp, P1 case. In addition, the higher temperature profile is continued in the flow direction for ramp case P1, compared to the increase in injection pressures representing that the combustion flame extends for a longer length due to the additional shocks emerging from the ramp base interfering with the fuel stream shear layers stream. Figure 15 represents the temperature variations at the bottom and top walls for different cases. The plot shows similar temperature peaks on the lower and top walls of the combustor which indicates that heat flux generated due to the combustion reaction transpires only at the centerline regime of the combustor. The enthalpy contours for various fuel injection pressures are depicted in Fig. 16. In contrast to P1, the increase in the enthalpy is continued in the flow direction of the combustor in the strut model, wherein an

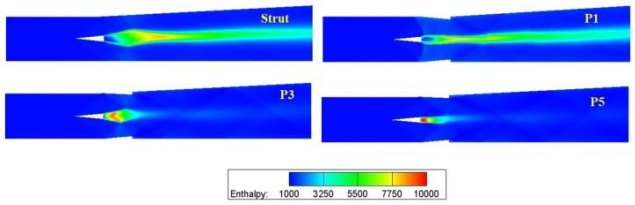

Fig. 16 Enthalpy contour for different models

enthalpy rise is apparent downstream of the strut injector. Since the ramp's location in the combustor, a reduction in enthalpy spread is noticed in P3 and P5, which, in contrast to prior models, implies a less rapid pace of heat release with an increase in injection pressure.

3.4 Mixing and Combustion Efficiencies

Mixing & combustion efficiencies are critical parameters for the effectiveness of scramjet combustor. Mixing efficiency is a ratio of stoichiometric H_2 mass flux to total H_2 mass flux.

$$\eta_{mix}(x) = \frac{\int_A \propto \rho u Y_{H_2} dA}{\int_A \rho u Y_{H_2} dA}$$

$$= \frac{\int_A \propto \rho u Y_{H_2} dA}{\dot{m}_{H_2(x)}} \quad \text{if, } \alpha = \begin{cases} 1, & \emptyset < 1 \\ \frac{1}{\emptyset}, & \emptyset \geq 1 \end{cases} \qquad (2)$$

Mixing efficiency distribution of basic strut & double ramps configured combustor model with various injection pressures are plotted in Fig. 17(a). Complete mixing is observed for the P5 case nearer to the injector itself, whereas for other cases mixing is complete at X=0.15m downstream of strut. This is due to an increase in H_2 jet pressure enhancing the fuel distribution which increases the mixing of fuel with incoming air.

A key parameter that is being used to examine the behaviour of scramjet combustors is combustion efficiency (Suppandipillai et al., 2021). The following equation is used to determine combustion efficiency:

$$\eta_c(x) = 1 - \frac{\int A(x)\rho_{gas} u Y_{H_2} dA}{\dot{m}_{H_{2(inj)}}} = 1 - \frac{\dot{m}_{H_{2(x)}}}{\dot{m}_{H_{2(inj)}}} \qquad (3)$$

Figure 17(b) shows mixing and combustion efficiency for different H_2 jet pressures to supersonic airflow. For the strut case, the whole combustion occurs at X=0.275m, however, for the ramp scenario with the injection pressure of 1 bar, the combustion is complete at X=0.25m it is due to the enhanced residence time of hydrogen-air mixing and combustion. An increase in the injection pressure, P5, reduces ignition delay and enhances combustion at a short combustor length of 0.12m which is about 52% less distance than the P1 configuration.

3.5 Total Pressure Loss

The injection pressures and oblique shocks created by the strut accelerate air-fuel mixtures, resulting in stagnation pressure loss. The following equation (Suppandipillai et al., 2021) has been used to determine

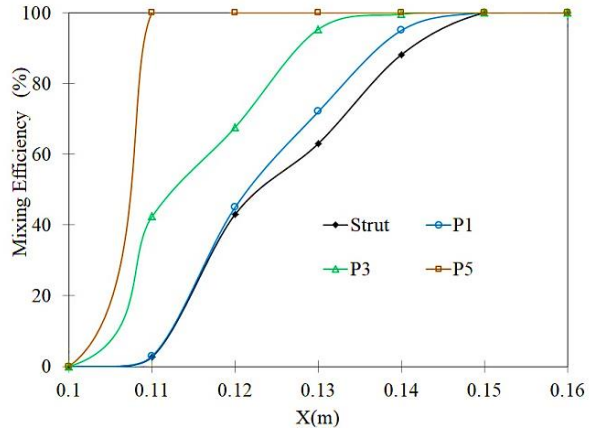

(a)

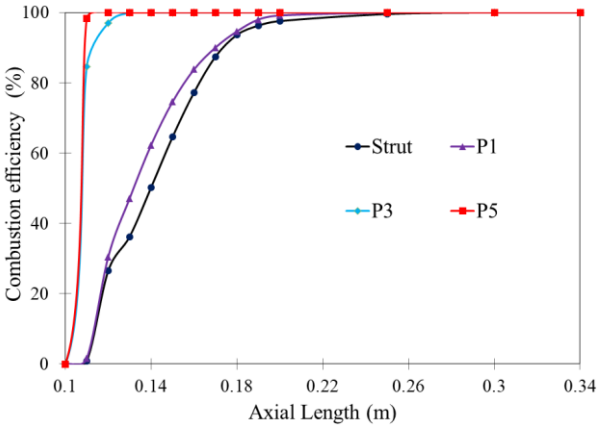

(b)

Fig. 17 (a) Mixing and (b) Combustion efficiencies of DLR strut scramjet combustor models with various injection pressures

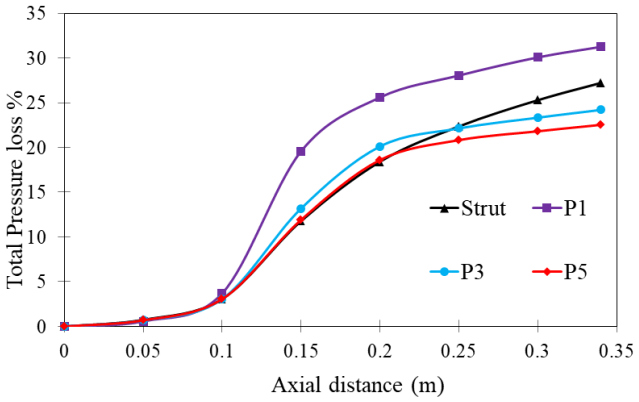

Fig. 18 Impact of injection pressure on total pressure loss in DLR strut scramjet combustor: A comparative analysis

pressure loss throughout the combustor. Stagnation pressure loss along a flow direction of models is plotted in Fig. 18. Total pressure loss is reported to be around 22.53% and 24.2% for ramp cases with hydrogen jet pressures of 5 bar and 3 bar respectively, it is due to weak shock generation and reflections in the combustor which could be observed from Fig. 5, and Fig.6. Further, the injection scheme P5, compared to the baseline model, results in nearly 17% less stagnation pressure loss in ramp configuration.

$$\eta_t = 1 - \frac{\int_A P_o \rho_u dA}{\int_A P_{oinl} \rho_u dA} \quad (4)$$

4. CONCLUSION

In a reactive flow condition, mixing and combustion of varying H_2 fuel jet pressure from a central strut injection combustor employing wall-mounted ramps has been computationally examined. Critical parameters such as wall static pressures, distribution of temperature at different locations of the combustor, mixing and combustion efficiencies based on H_2 mass fraction, & overall pressure loss across the combustor are utilized to estimate the effectiveness of ramps downstream of the strut. The following findings are drawn from this investigation:

- The numerical shadowgraph explains the addition of shocks from the ramp influences parametric variations inside the combustor. Due to variable jet pressure, the intensity of shock wave interaction varies for different cases.
- For the ramp with P= 1 bar, the lambda-type shock patterns are generated due to the separation of the boundary layer before the leading edge of ramps and flow gets decelerated downstream of the strut injector. Additional vortices are formed for the ramp case which helps in holding the flame to enhance combustion. An increase in hydrogen jet pressure for the ramp cases accelerates flow downstream of the injection location.
- Hydrogen air mixing & complete combustion is accelerated with an increase in hydrogen jet pressure within a short combustor length. Compared to the DLR scramjet model, the P5 injection pressure achieves complete fuel & air combustion within a combustor length that is reduced by 52%.
- For ramp cases with jet pressures of 3 bar and 5 bar, the minimum pressure loss across the combustors is noted, due to less intense oblique shocks compared to other cases. A reduction in pressure drop by 17% is observed for the injection pressure P5 compared to the baseline model. Further studies on fuel injection upstream of the ramps, aimed at enhancing heat flux in the lateral direction, are considered for future investigation.

CONFLICT OF INTEREST

The authors declare no conflicts of interest.

AUTHORS CONTRIBUTION

A. Antony Athithan: Investigation. **S. Jeyakumar:** Investigation, Writing – review & editing.

REFERENCES

Abu-Farah, L., Haidn, O. J., & Kau, H. P. (2014). Numerical simulations of single and multi-staged injection of H2 in a supersonic scramjet combustor. *Propulsion and Power Research*, *3*(4), 175–186. https://doi.org/10.1016/j.jppr.2014.12.001

Antony Athithan, A., Jeyakumar, S., & Poddar, S. (2021). Influence of wall mounted ramps on DLR strut scramjet combustor under non-reacting flow field. *Materials Today: Proceedings*. https://doi.org/https://doi.org/10.1016/j.matpr.2021.11.347

Aravind, S., & Kumar, R. (2019). Supersonic combustion of hydrogen using an improved strut injection scheme. *International Journal of Hydrogen Energy*, *44*(12), 6257–6270. https://doi.org/10.1016/j.ijhydene.2019.01.064

Assis, S. M., Jeyakumar, S., & Jayaraman, K. (2019). The effect of transverse injection upstream of an axisymmetric aft wall angled cavity in a supersonic flow field. *Journal of Physics: Conference Series*, *1276*(1). https://doi.org/10.1088/1742-6596/1276/1/012019

Athithan, A. A., & Jeyakumar, S. (2022). Numerical investigations on the influence of double ramps in a strut based scramjet combustor. *International Journal of Engine Research*, *0*(0), 14680874221107136. https://doi.org/10.1177/14680874221107137

Athithan, A. A., Jeyakumar, S., Sczygiol, N., Urbanski, M., & Hariharasudan, A. (2021). The combustion characteristics of double ramps in a strut-based scramjet combustor. *Energies*, *14*(4), 831. https://doi.org/10.3390/en14040831

Ben-Yakar, A., & Hanson, R. K. (2001). Cavity flame-holders for ignition and flame stabilization in scramjets: An overview. *Journal of Propulsion and Power*, *17*(4), 869–877. https://doi.org/10.2514/2.5818

Bruno, C., & Ingenito, A. (2021). Some key issues in hypersonic propulsion. *Energies*, *14*(12). https://doi.org/10.3390/en14123690

Cecere, D., Giacomazzi, E., & Ingenito, A. (2014). A review on hydrogen industrial aerospace applications. *International Journal of Hydrogen Energy*, *39*(20), 10731–10747. https://doi.org/10.1016/j.ijhydene.2014.04.126

Chang, L., Yang, C., Su, X., Dai, X., Xu, Q., & Guo, L. (2024). Investigations on affinity law under gas–liquid conditions in multistage radial and mixed-flow multiphase pumps. *International Journal of Fluid Engineering*, *1*(1). https://doi.org/10.1063/5.0191201

Choubey, G., Solanki, M., Bhatt, T., Kshitij, G., Yuvarajan, D., & Huang, W. (2023). Numerical investigation on a typical scramjet combustor using cavity floor H2 fuel injection strategy. *Acta Astronautica*, *202*, 373–385. https://doi.org/https://doi.org/10.1016/j.actaastro.2022.10.055

Clark, R. J., & Bade Shrestha, S. O. (2015). A review of numerical simulation and modeling of combustion in scramjets. *Proceedings of the Institution of Mechanical Engineers, Part G: Journal of Aerospace Engineering*, *229*(5), 958–980. https://doi.org/10.1177/0954410014541249

Doster, J. C., King, P. I., Gruber, M. R., & Maple, R. C. (2007). *Pylon fuel injector design for a scramjet combustor*. AIAA Paper 2007-5404.

Fureby, C., Fedina, E. & Tegnér, J. (2014). A computational study of supersonic combustion behind a wedge-shaped flameholder. *Shock Waves*, *24*, 41–50. https://doi.org/10.1007/s00193-013-0459-2

Gao, J., Yuan, Z., Hou, Y., & Chen, W. (2024). Numerical study on the influence of plugging rate on the performance of adjustable steam ejector. *International Journal of Fluid Engineering*, *1*(2). https://doi.org/10.1063/5.0204421

Génin, F., & Menon, S. (2010). Simulation of turbulent mixing behind a strut injector in supersonic flow. *AIAA Journal*, *48*(3), 526–539. https://doi.org/10.2514/1.43647

Gerlinger, P., & Bruggemann, D. (2000). Numerical investigation of hydrogen strut injections into supersonic airflows. *Journal of Propulsion and Power*, *16*(1), 22–28. https://doi.org/10.2514/2.5559

Goyne, C. P., McDaniel, J. C., Quagliaroli, T. M., Krauss, R. H., & Day, S. W. (2001). Dual-mode combustion of hydrogen in a Mach 5, continuous-flow facility. *Journal of Propulsion and Power*, *17*(6), 1313–1318. https://doi.org/10.2514/2.5880

Gruber, M. R., Carter, C. D., Montes, D. R., Haubelt, L. C., King, P. I., & Hsu, K. Y. (2008). Experimental studies of pylon-aided fuel injection into a supersonic crossflow. *Journal of Propulsion and Power*, *24*(3), 460–470. https://doi.org/10.2514/1.32231

Guerra, R., Waidmann, W., & Laible, C. (1991). An experimental investigation of the combustion of a hydrogen jet injected parallel in a supersonic air stream. *AIAA Paper 91-5102*. https://doi.org/10.2514/6.1991-5102

Huang, W. (2014). Design exploration of three-dimensional transverse jet in a supersonic crossflow based on data mining and multi-objective design optimization approaches. *International Journal of Hydrogen Energy*, *39*(8), 3914–3925. https://doi.org/10.1016/j.ijhydene.2013.12.129

Huang, W. (2015). Investigation on the effect of strut configurations and locations on the combustion performance of a typical scramjet combustor. *Journal of Mechanical Science and Technology*, *29*(12), 5485–5496. https://doi.org/10.1007/s12206-015-1150-6

Huang, W., Luo, S. Bin, Liu, J., & Wang, Z. G. (2010).

Effect of cavity flame holder configuration on combustion flow field performance of integrated hypersonic vehicle. *Science China Technological Sciences*, *53*(10), 2725–2733. https://doi.org/10.1007/s11431-010-4062-9

Huang, W., Wang, Z. G., Li, S. Bin, & Liu, W. D. (2012). Influences of H2O mass fraction and chemical kinetics mechanism on the turbulent diffusion combustion of H2-O2 in supersonic flows. *Acta Astronautica*, *76*, 51–59. https://doi.org/10.1016/j.actaastro.2012.02.017

Huang, W., Wu, H., Yang, Y. guang, Yan, L., & Li, S. bin. (2020). Recent advances in the shock wave/boundary layer interaction and its control in internal and external flows. *Acta Astronautica*, *174*(May), 103–122. https://doi.org/10.1016/j.actaastro.2020.05.001

Ivanova, E. M., Noll, B. E., & Aigner, M. (2013). A numerical study on the turbulent schmidt numbers in a jet in crossflow. *Journal of Engineering for Gas Turbines and Power*, *135*(1), 1–10. https://doi.org/10.1115/1.4007374

Jeyakumar, S., Assis, S. M., & Jayaraman, K. (2017). Experimental study on the characteristics of axisymmetric cavity actuated supersonic flow. *Proceedings of the Institution of Mechanical Engineers, Part G: Journal of Aerospace Engineering*, *231*(14), 2570–2577. https://doi.org/10.1177/0954410016667149

Jeyakumar, S., Assis, S. M., & Jayaraman, K. (2018). Effect of axisymmetric aft wall angle cavity in supersonic flow field. *International Journal of Turbo and Jet Engines*, *35*(1), 29–34. https://doi.org/10.1515/tjj-2016-0027

Jeyakumar, S., Balachandran, P., & Indira, S. (2006). Experimental investigations on supersonic stream past axisymmetric cavities. *Journal of Propulsion and Power*, *22*(5), 1141–1144. https://doi.org/10.2514/1.21024

Jeyakumar, S., Kandasamy, J., Karaca, M., Karthik, K., & Sivakumar, R. (2021). Effect of hydrogen jets in supersonic mixing using strut injection schemes. *International Journal of Hydrogen Energy*, *46*(44), 23013–23025. https://doi.org/https://doi.org/10.1016/j.ijhydene.2021.04.123

Kumaran, K., & Babu, V. (2009). Investigation of the effect of chemistry models on the numerical predictions of the supersonic combustion of hydrogen. *Combustion and Flame*, *156*(4), 826–841. https://doi.org/10.1016/j.combustflame.2009.01.008

Lakka, S., Randive, P., & Pandey, K. M. (2021). Implication of geometrical configuration of cavity on combustion performance in a strut-based scramjet combustor. *Acta Astronautica*, *178*, 793–804. https://doi.org/10.1016/j.actaastro.2020.08.040

Lee, S. (2012). Mixing Augmentation with Cooled Pylon Injection in a Scramjet Combustor. *Journal of Propulsion and Power*, *28*(3), 477–485. https://doi.org/10.2514/1.B34220

Li, Z., & Gu, H. (2022). Investigation for effects of jet scale on flame stabilization in scramjet combustor. *Energies*, *15*(10). https://doi.org/10.3390/en15103790

Liu, J. L., & Zhu, A. M. (2024). Bi-reforming with a ratio of CH4/CO2/H2O = 3/1/2 by gliding arc plasma catalysis for power to fuels. *International Journal of Fluid Engineering*, *1*(2). https://doi.org/10.1063/5.0197581

Liu, M., Sun, M., Yang, D., Zhao, G., Tang, T., An, B., & Wang, H. (2023). Mixing and combustion characteristics in a scramjet combustor with different distances between cavity and backward-facing step. *Chinese Journal of Aeronautics*. https://doi.org/https://doi.org/10.1016/j.cja.2023.04.013

Magnussen, B. F., & Hjertager, B. H. (1976). On mathematical models of turbulent combustion with special emphasis on soot formation and combustion. *16th Symposium (International) on Combustion,The Combustion Institute*, *16*(1), 719–729. https://doi.org/doi:10.1016/S0082-0784(77)80366-4

Moorthy, J. V. S., Rajinikanth, B., Charyulu, B. V. N., & Amba Prasad Rao, G. (2014). Effect of ramp-cavity on hydrogen fueled scramjet combustor. *Propulsion and Power Research*, *3*(1), 22–28. https://doi.org/10.1016/j.jppr.2014.01.001

Muhammed, I., N, S. B., Suryan, A., Lijo, V., Simurda, D., & Kim, H. D. (2024). Computational study of flow separation in truncated ideal contour nozzles under high-altitude conditions. *International Journal of Fluid Engineering*, *1*(1). https://doi.org/10.1063/5.0190399

Neill, S. M., & Pesyridis, A. (2017). Modeling of supersonic combustion systems for sustained hypersonic flight. *Energies*, *10*(11). https://doi.org/10.3390/en10111900

Oevermann, M. (2000). Numerical investigation of turbulent hydrogen combustion in a SCRAMJET using flamelet modeling. *Aerospace Science and Technology*, *4*(7), 463–480. https://doi.org/10.1016/S1270-9638(00)01070-1

Ou, M., Yan, L., Huang, W., Li, S. bin, & Li, L. quan. (2018). Detailed parametric investigations on drag and heat flux reduction induced by a combinational spike and opposing jet concept in hypersonic flows. *International Journal of Heat and Mass Transfer*, *126*, 10–31. https://doi.org/10.1016/j.ijheatmasstransfer.2018.05.013

Qin, Q., Agarwal, R., & Zhang, X. (2019). A novel method for flame stabilization in a strut-based scramjet combustor. *Combustion and Flame*, *210*, 292–301. https://doi.org/10.1016/j.combustflame.2019.08.038

Soni, R. K., & De, A. (2017). Investigation of strut-ramp

injector in a Scramjet combustor: Effect of strut geometry, fuel and jet diameter on mixing characteristics. *Journal of Mechanical Science and Technology*, *31*(3), 1169–1179. https://doi.org/10.1007/s12206-017-0215-0

Suneetha, L., Randive, P., & Pandey, K. M. (2019). Numerical investigation on implication of dual cavity on combustion characteristics in strut based scramjet combustor. *International Journal of Hydrogen Energy*, *44*(60), 32080–32094. https://doi.org/10.1016/j.ijhydene.2019.10.064

Suppandipillai, J., Kandasamy, J., Sivakumar, R., Karaca, M., & K, K. (2021). Numerical investigations on the hydrogen jet pressure variations in a strut based scramjet combustor. *Aircraft Engineering and Aerospace Technology*, *93*(4), 566–578. https://doi.org/10.1108/AEAT-08-2020-0162

Tahani, M., Hojaji, M. and Mahmoodi Jezeh, S. V. (2016). Turbulent jet in crossflow analysis with LES approach. *Aircraft Engineering and Aerospace Technology*, *88*(6), 717–728. https://doi.org/https://doi.org/10.1108/AEAT-10-2014-0167

Thakur, A., Thillai, N., & Sinha, A. (2021). Combustion enhancement in rearward step based scramjet combustor by air injection at step base. *Propulsion and Power Research*, *10*(3), 224–234. https://doi.org/10.1016/j.jppr.2021.09.003

Viaud, L., & Mestre, A. (1966). Application of supersonic combustion to ramjets. *Aircraft Engineering and Aerospace Technology*, *38*(2), 15–17. https://doi.org/http://dx.doi.org/10.1108/eb034121

Waidmann, W., Alff, F., Böhm, M., Brummund, U., Clauß, W., & Oschwald, M. (1995). Supersonic combustion of hydrogen/air in a scramjet combustion chamber. *Space Technology*, *15*(6), 421–429.

Waidmann, W., Alff, F., Brummund, U., Bohm, M., Clauss, W., & Oschwald, M. (1994). Experimental investigation of the combustion process in a supersonic combustion ramjet (Scramjet). *Jahrestagung, Erlangen, Germany: DGLR*, 62 9-38.

Wang, T., Li, G., Yang, Y., Wang, Z., Cai, Z., & Sun, M. (2020). Combustion modes periodical transition in a hydrogen-fueled scramjet combustor with rear-wall-expansion cavity flameholder. In *International Journal of Hydrogen Energy* (Vol. 45, Issue 4, pp. 3209–3215). https://doi.org/10.1016/j.ijhydene.2019.11.118

Xi, W., Xu, M., Liu, C., Liu, J., & Sunden, B. (2022). Generation and propagation characteristics of an auto-ignition flame kernel caused by the oblique shock in a supersonic flow regime. *Energies*, *15*(9). https://doi.org/10.3390/en15093356

Xue, R., Wei, X., He, G., Hu, C., & Tang, X. (2017). Effect of parallel-jet addition on the shock train characteristics in a central-strut isolator by detached eddy simulation. *International Journal of Heat and Mass Transfer*, *114*, 1159–1168. https://doi.org/10.1016/j.ijheatmasstransfer.2017.06.074

Zhang, J., Feng, G., Bai, H., Lv, K., & Bao, W. (2023). Research on combustion characteristics of scramjet combustor with different flight dynamic pressure conditions. *Propulsion and Power Research*, *12*(1), 69–82. https://doi.org/10.1016/j.jppr.2023.02.006

Zhang, R. rui, Huang, W., Li, L. quan, Yan, L., & Moradi, R. (2018). Drag and heat flux reduction induced by the pulsed counterflowing jet with different periods on a blunt body in supersonic flows. *International Journal of Heat and Mass Transfer*, *127*, 503–512. https://doi.org/10.1016/j.ijheatmasstransfer.2018.08.066